

Application of imaging techniques to objectify *Finger Tapping Test* used in the diagnosis of Parkinson's disease

Jacek JAKUBOWSKI¹ , Anna POTULSKA-CHROMIK² , Jolanta CHMIELIŃSKA¹ ,
Monika NOJSZEWSKA² , and Anna KOSTERA-PRUSZCZYK² 

¹ Faculty of Electronics, Military University of Technology, Warsaw, Poland

² Department of Neurology, Medical University of Warsaw, Warsaw, Poland

Abstract. Finger tapping is one of the standard tests for Parkinson's disease diagnosis performed to assess the motor function of the patient's upper limbs. In clinical practice, the assessment of the patient's ability to perform the test is carried out visually and largely depends on the experience of clinicians. This article presents the results of research devoted to the objectification of this test. The methodology was based on the proposed measurement method consisting of frame processing of the video stream recorded during the test to determine the time series representing the distance between the index finger and the thumb. Analysis of the resulting signals was carried out in order to determine the characteristic features that were then used in the process of distinguishing patients with Parkinson's disease from healthy cases using methods of machine learning. The research was conducted with the participation of 21 patients with Parkinson's disease and 21 healthy subjects. The results indicate that it is possible to obtain the sensitivity and specificity of the proposed method at the level of approx. 80%. However, the patients were in the so-called ON phase when symptoms are reduced due to medication, which was a much greater challenge compared to analyzing signals with clearly visible symptoms as reported in related works.

Key words: image processing; medical diagnosis; Parkinson's disease; finger-tapping test.

1. INTRODUCTION

Finger Tapping or Rapid Finger Tapping (RFT) is the name of a typical test performed in the diagnosis of Parkinson's disease (PD) to assess the slowness and disturbances in the continuity of finger movement occurring in the disease [1]. According to the test, the subjects are asked to tap the index finger and thumb together ten times making as large, rapid and smooth movement as possible. In clinical practice, this motor task performed by the patient is assessed taking into account speed, amplitude and its decrease over time, as well as hesitations and stops of movement. During the medical interview, the clinician evaluates all of the above features of movement by a natural visual inspection and rates them with a single integrated result using contemporary medical standards for the diagnosis and assessment of the severity of Parkinson's disease symptoms known as the UPDRS (Unified Parkinson's Disease Rating Scale) which was introduced in 1987 [2, 3]. The standard uses an ordinal scale with only five-step categories to assess four components or parts including the intellectual condition and mood disorders (part I), the quality of everyday life (part II), movement functions (part III) and motor complications (part IV). The Fin-

ger Tapping is assessed within part III together with speech, facial expressions, tremors, gait, posture, getting up from a chair, etc. The UPDRS score in this part is the sum of the grades of all of them. Higher scale ranges correspond to more advanced stages of the disease. However, the use of the scale requires a good knowledge of the symptoms of the disease and extensive clinical experience of the examining medical doctors. In the RFT test the accuracy of the assessment may be compromised because of the subjectivity and the difficulty to detect slight changes in the movement of the patient's fingers properly. Hence the need to develop objective finger-tapping measurements and processing. From an engineering point of view, the RFT is an ordinary movement and as such, it can be accurately quantified and analyzed using technical tools. The methods used for this purpose fall into two categories: wearable sensors composed of accelerometers or gyroscopes and image sensors based on video processing. A survey of real-time sensing and modelling of the human body used to pose estimation of hands can be found in [4]. The choice of the technology for the objectification of the Finger Tapping Test should be dictated by simplicity, which gives the potential opportunity to assess people during remote consultations when they are at home and the doctor in his office receives the necessary results. This is particularly important for the development of remote medicine in the diagnosis of Parkinson's disease. As the wearable sensors should be directly attached to fingers, which is disturb-

*e-mail: jacek.jakubowski@wat.edu.pl

Manuscript submitted 2022-07-26, revised 2023-02-10, initially accepted for publication 2023-02-15, published in April 2023.

ing due to connecting wires, and require additional mobile devices [5–8], they are usually intended for use in lab settings. Because of that, in this paper, we propose a video-based approach and examine quantitatively its possibility for proper classification between patients with Parkinson’s disease and healthy subjects. A method was developed for converting redundant image data acquired by a single camera into simpler representations that facilitate data interpretation and the effective use of machine learning algorithms. The method consists in mapping the movement occurring in RFT into a time series representing the distance between the index finger and the thumb changing in time. In order to detect and track landmarks of interest, passive markers of a uniform color were placed on the participant’s fingers.

2. RELATED WORKS

The concept of using a video-based motion method to objectify the RFT test and to find new digital biomarkers in this way is not new and has attracted the attention of many scientific centers for several years. One of the first attempts was presented by Krupicka *et al.* in 2011 [9]. They proposed the use of a time series representing the distance between the fingers. This series was obtained by using a motion capture system based on two cameras, which analyzed the position of light passive and wireless reflexive markers attached to fingers. To capture the movement of the fingers it was necessary to illuminate the scene with infrared emitters. However, the authors limited themselves only to the presentation of the hardware solution itself and they did not report the results of studies using any cohort of patients. Research with patients and with the use of a more advanced motion capture system that was based on 12 cameras and lightweight infrared emitting diodes was presented by Lainscsek *et al.* in [10]. The advantage of their system was the precise determination of the distance between the diodes in millimeters and the disadvantage was occlusive artifacts that occurred when fewer than two cameras detected any of the IR markers. They modeled recorded time waveforms of 10 s length using differential equations. Six parameters of the model were used as motion descriptors. The ability to discriminate patients and control subjects was investigated in two groups differing in standard deviations in age and UPDRS score. Signals coming from the dominant hands were recorded in the research. Extremely different sensitivity values (0.95 vs. 0.57) and specificity (0.83 vs. 0.79) in both groups were obtained but this study had the limitation that the total number of participants was very small. There were merely six and seven positively diagnosed patients in the first and second groups, respectively. Because of that leave-one-out cross-validation was used [11]. A more extended classification study was performed by Khan *et al.* in [12]. In this work, a high recognition accuracy of 95.8% was reported and obtained on the basis of the analysis of 471 instances coming from the dominant hand which appeared to be right for all participants. Unlike in other articles, a single camera with a fully non-invasive, i.e. without any kind of markers method of im-

age processing, was used. The method was based on a motion segmentation algorithm consisting of comparing the incoming video frame to a previously referenced frame and was shown to be almost the same as a method in which the movement was mapped by tracking colored markers placed on the fingers. In order to make the amplitude of the tapping signal independent of the distance of the hand from the camera, they adopted a novel calibration approach motivated by the observation that the height of an adult person’s face is approximately equal to the length of that person’s hand. The recognition was based on the SVM classifier and 15 signal features extracted directly from the time waveforms. However, the paper presents rather a classification of signals because the data pool containing 471 instances was obtained from only 13 patients and six healthy cases. In 2020 we also used one camera for image acquisition and presented pilot studies devoted to the detection of color markers attached to the subject’s fingers in order to demonstrate the possibility of using spectral analysis for quantitative descriptions of the tapping signals [13]. The most advanced paper concerning the concept of a video-based system to measure various types of movement assessed in Parkinson’s disease, including finger tapping, was published by Monje *et al.* in 2021 [14]. In their fully non-invasive system, a single web camera was used with software based on one dedicated convolutional neural network to detect hands and the other to determine specific landmarks corresponding to the joints and tips of the fingers [15, 16]. They acquired signals obtained from 22 patients and from 20 healthy cases. Based on features describing jointly left- and right-hand signals and using the cross-validation technique, they achieved average values of sensitivity and specificity of up to 73% and 80%, respectively.

3. PROBLEM STATEMENT

In the related papers presented above, the authors report that participants took part in the research without having taken their anti-parkinsonian medications for several hours (the OFF phase). However, making a diagnosis in the presence of clearly visible clinical symptoms is not difficult for a medical doctor. The real problem is the correct diagnosis at an early stage of the disease when the severity of classic symptoms is small. It is estimated that incorrect diagnosis may occur in about 10–25% of cases [17, 18]. This paper presents the results of research on the video-based objectification of RFT using a research group of patients who were in the so-called switched-ON phase. The ON phase is the action phase of drugs that reduce the symptoms of the disease. Persons in this phase resemble patients described by the lower range of the UPDRS scale, which corresponds to patients with low severity of symptoms, characteristic of the early stage of the development of the disease. The practice of using patients in the ON phase for research on the construction of a diagnostic system is not new and has been used for several years, mainly in the case of using voice samples and handwriting in the analysis [19–22]. Data from patients in the ON phase pose a much greater challenge for data processing methods, but

at the same time, the results obtained with their help may be of greater value for the development of new diagnostic methods, which should recognize the disease at an early stage of its development. In addition, it should be stated that Parkinson's disease can affect the left, right or both sides of the body and the question arises which hand should be taken into account when recording tapping data – the more affected side, the less affected side or both sides. The question is especially important when the affected side is not known before diagnosis. The dominant hand was selected in advance in some papers. Therefore, in this work, a certain method was proposed and verified and was aimed at automatically indicating this hand, whose RFT should be taken into account in the classification process.

4. DATA POOL AND ACQUISITION PROTOCOL

The data for analysis were obtained as part of clinical trials conducted under the supervision of specialists in the field of neurology in the Department of Neurology at the Medical University of Warsaw in Poland. The developed procedure for collecting RFT data assumed the same conditions of using a digital camera for all participants. During data acquisition, a person reporting for the examination at a dedicated doctor's office sat on a chair, whose distance from the camera, given the constant focal length of its lens, was constant and determined using markers applied on the floor. The tests were carried out in accordance with the recommendations contained in [2]. The participants were asked to tap their fingers of the right and left hands successively at their own tempo, but as quickly as possible and with the greatest possible movement range – Fig. 1. The time to test each hand was about 15 s so that video recordings of the same length of 10 s could be used for further analysis. The Bioethics Committee approved the research protocol and the participants were informed about its scope and provided written consent before the study. A total of 48 people took part in the research; however, some videos had to be rejected because it turned out that in these cases the tapping fingers got out of the camera field of view during acquisition. Eventually, 21 videos were obtained from the PD patients. The health control (HC) group also included 21 people. They were examined by clinicians to make sure there had been no movement disorders or injuries that could affect the motor function of the hands. The basic clinical features and demographic characteristics of patients in the PD and HC groups are presented in Table 1.

Table 1

Baseline characteristics of PD and HC participants

group	PD	HC
general		
total	21	21
age	60 ± 16	41 ± 15
UPDRS part III	26 ± 10	–
gender		
female	14	5
male	7	16
more affected side		
right	8	–
left	5	–
both	8	–

5. IMAGE TO SIGNAL CONVERSION

According to the adopted concept of data acquisition, during the rapid Finger Tapping Test (RFT) a video stream was recorded using a traditional color camera. The study used the Basler acA1440-220uc, which includes the IMX273 CMOS image sensor delivering 227 frames per second at 1.6 MP resolution. During the recording, the optimal acquisition rate of 60 fps was used. It was large enough to eliminate the effects of blurring markers on individual frames, as shown in Fig. 1, and at the same time small enough to determine the exposure time giving the opportunity to obtain the right contrast to carry out segmentation. Segmentation was done by binarizing the color image using the information contained in individual color channels. Figure 2 presents an example of an image from the recorded video stream during the subject's performance of the rapid tapping test and its components in individual color channels I_R , I_G , I_B . In a monochrome image, the higher the value of a pixel, the brighter it is. In addition, each component image was subjected to a contrast improvement process, relying on stretching the histogram. The color of the markers used was bright yellow. This color is characterized by extreme values in the channels I_G and I_B , which made it easier to create a binary image I_{BIN} based



Fig. 1. Sequence of video frames during the RFT test when the acquisition rate was set to 60 fps (every second frame is visible)



Fig. 2. Single color frame and its decomposition into RGB channels

on the formula (1):

$$I_{BIN}(x,y) = \begin{cases} 0 & \text{for } (x,y): (I_G(x,y) > T_G) \text{ and} \\ & (I_B(x,y) < T_B), \\ 255 & \text{for the rest of } (x,y) \end{cases} \quad (1)$$

in which x and y specify the coordinates of the pixel. Thresholds T_G and T_B have been selected in an experimental way so that in the binary image the areas corresponding to the markers are indicated. The above binarization should ensure that points are obtained on the plane, the location of which corresponds to the tips of the fingers. However, the result of binarization shown in Fig. 3 indicates the existence of many artifacts related to the presence of colors in the image with similar pixel values in color channels G and B . The nature of the artifacts is similar to “salt & pepper” noise, so it can be easily eliminated using median filtration. Figure 4 shows the result of such filtration with a filter with a square mask of dimension 20. The next step is to determine the coordinates of the position in the binary image of the markers placed on the index finger and thumb. For this purpose, the k -means algorithm was used, which allows assigning data to classes with a given number and indicating the

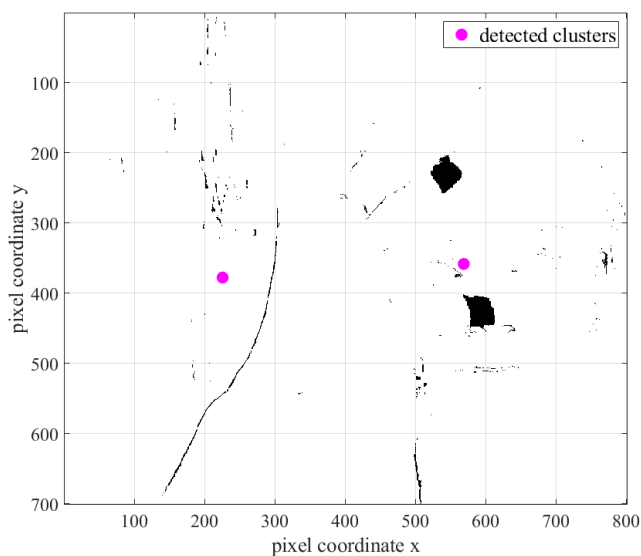


Fig. 3. Binary image corresponding to formula (1) with clusters wrongly detected (magenta points). The real fingertips are represented by the black blobs

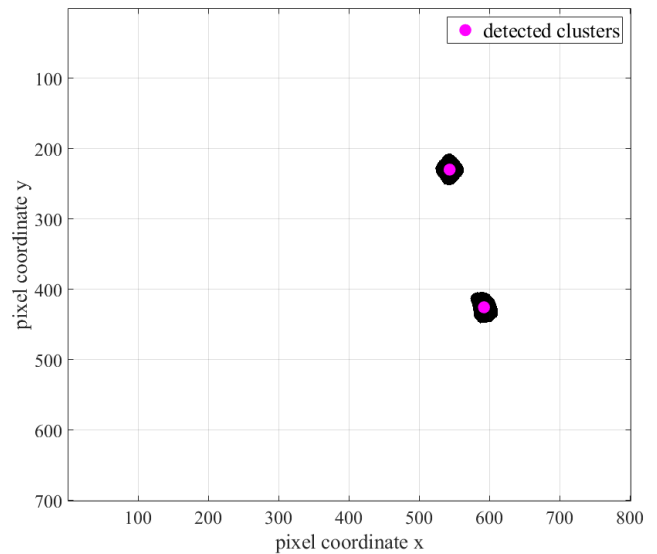


Fig. 4. Results of median filtration of the binary image depicted in Fig. 3 (properly detected clusters)

centers of created clusters. In the task of detecting two markers, the data must be divided into two groups. Figures 3 and 4 show the detection effect for binary images before and after median filtration. Correct indication of centers and representing them with points $p_1(x_1, y_1)$ and $p_2(x_2, y_2)$ allows us to determine the Euclidean distance (2) between the index finger and thumb:

$$D(p_1, p_2) = \sqrt{(x_2 - x_1)^2 + (y_2 - y_1)^2}. \quad (2)$$

Due to the fact that the coordinates of the centers in binary images are determined by the number of pixels in the horizontal and vertical directions, the distance determined by (2) is also expressed in pixels. In order to obtain the time waveform of the relative movement of the fingers of the test subject, the procedure should be repeated for each frame from the recorded video sequence. Figure 5 shows the waveforms obtained in this way for the right and left hand of a patient who has been diagnosed with the classic form of Parkinson’s disease with the more affected side on the left. The patient was rated for the UPDRS movement component at level 24. Obtaining the waveforms of changes in the distance between the fingers allows an objective assessment of the nature of their movement.

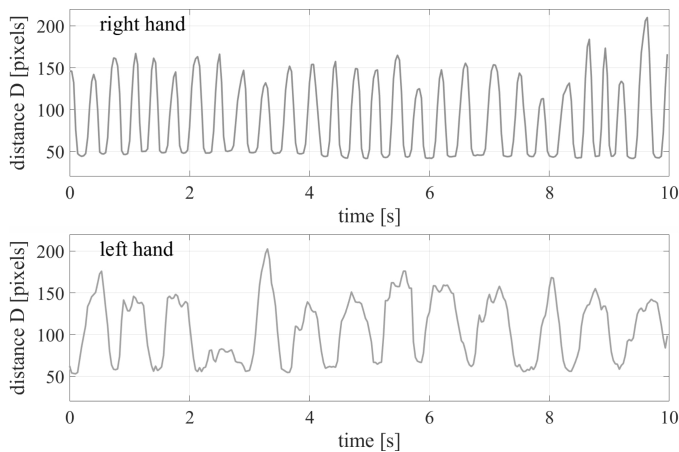


Fig. 5. Waveforms representing distances between fingers in the RFT test for each hand of a PD patient with more affected side left

6. FEATURE GENERATION

Based on domain knowledge about the motor functions of the upper limbs manifesting Parkinson's symptoms, it is possible to indicate certain numerical parameters of the obtained distance waveforms (2), which will quantitatively describe the rapid Finger Tapping Test. In this paper, a total of four characteristics describing waveforms of 10 s long were used, successively in the domain of signal values and in the frequency domain.

6.1. Features in the domain of values

The observed differences in the regularity of movement between the PD study group for symptomatic limbs and the control groups are the cause of differences in histograms of values. Figure 6 shows a histogram of an example signal of 10 s long acquired during the RFT test of the limb with Parkinsonian symptoms.

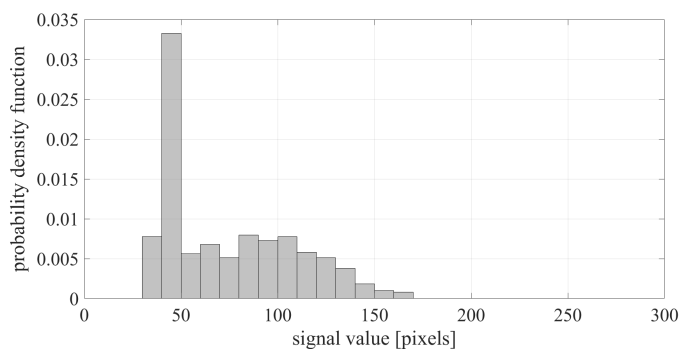


Fig. 6. Histogram of 10 second waveform values acquired during the RFT test of the affected hand of a PD patient (the sum of the fields of all rectangles is equal to one)

The histogram has been normalized in such a way as to satisfy the properties of the probability density function, i.e. the sum of the fields of all rectangles is equal to one. Analyzing this histogram, you can see a huge peak corresponding to small signal values. This peak indicates an extended time of holding the joined fingers before they are opened by the PD patient during

the RFT test and can be interpreted as caused by the occurrence of motor function disorders. The nature of the sample histogram with the same normalization obtained from one of the people from the HC group, presented in Fig. 7, is completely different. The regularity of the movement makes the number of signal values corresponding to the connected and disconnected fingers similar. The histogram is more symmetrical but much more deviates in shape from the normal distribution than the histogram for a PD patient depicted in Fig. 6. The above characteristics of histograms can be quantitatively described by skewness, which should be equal to zero for symmetric distributions, and kurtosis, which should tend to equal three for distributions close to normal. In the case of the histograms presented in Figs. 6 and 7, the values of the skewness and kurtosis pairs are [0.65 2.24] and [0.09 1.25], respectively.

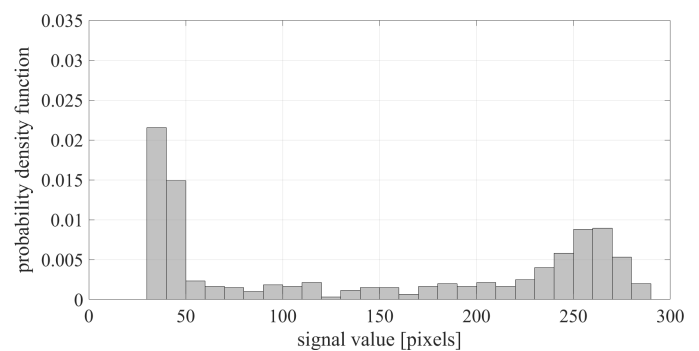


Fig. 7. Histogram of waveform values acquired during the RFT test of one hand of a HC subject (the sum of the fields of all rectangles is equal to one)

6.2. Features in the domain of spectra

The slowdowns observed among patients with Parkinson's disease are visible in the rapid tapping test in the form of a reduced frequency of movement, which can be determined from the spectrum of the distance signal (2) changing in time. Figure 8 shows magnitudes of the Fourier transforms of signals obtained from exemplary patients in the PD research group with both and right side affected, respectively and from a person belonging to the HC control group. The spectra were determined from signals with a duration of 10 s using the regular FFT algorithm. The mean of each signal was removed before the transform. To minimize the leakage effect in the spectral analysis, the Hanning window was used. In order to increase the resolution in the frequency domain, the original signals consisting of 600 samples were zero-padded up to the length of 4,096. It is easy to observe that the spectrum maxima corresponding to signals obtained from PD patients occur at a lower frequency as compared to the signal obtained from an HC person. The magnitude spectrum can also be used to quantify changes in the frequency of movement during the test. Such changes are characteristic of patients in the PD group and can be determined by a measure expressing spectrum broadening. Both parameters, i.e. the average frequency of motion and the measure of the width of the magnitude spectrum, can be obtained as part of a unified description based on spectral moments [23]. The idea

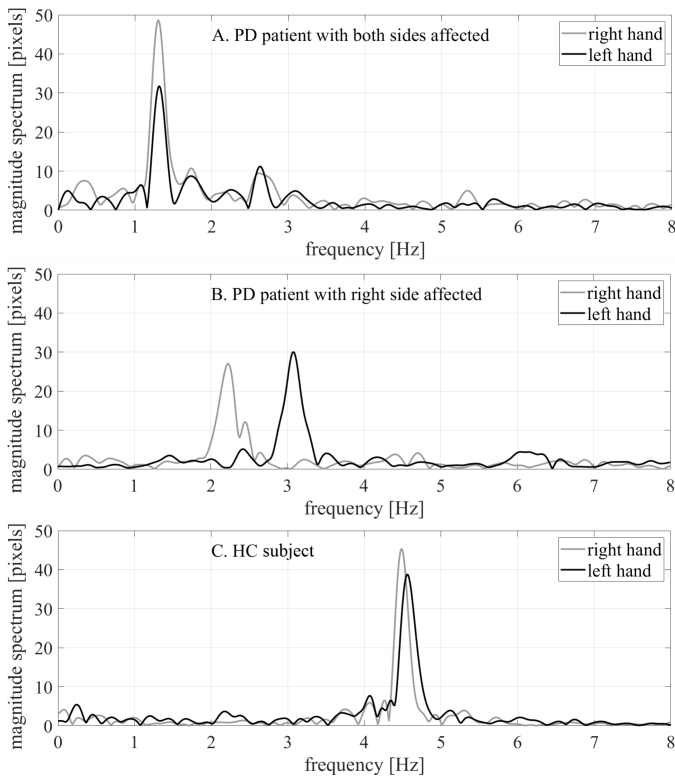


Fig. 8. Magnitudes of the Fourier transforms of RFT signals acquired for both hands in the case of a: PD patient with both sides affected (A), patient with right side affected (B) and HC subject (C)

behind this description is to treat the magnitude of a discrete spectrum $S(l)$, where l denotes frequency lines or bins changing from 1 to $N/2$ and N is the length of the discrete spectrum, as the probability density function of a certain random variable L . To fulfill the properties of a probability density function, the magnitude spectrum $S(l)$ should be normalized according to the formula:

$$S'(l) = \frac{S(l)}{\sum_{l=1}^{N/2} S(l)}. \quad (3)$$

Thanks to that the description $S'(l)$ is characterized by the property:

$$\sum_{l=1}^{N/2} S'(l) = 1, \quad (4)$$

which is specific to a probability density function of a certain random variable L . Using the common moment definitions, the quantitative characteristics of the spectrum, i.e. m_1 – the center of gravity and m_2 – the measure of the spectrum broadening can be determined as follows:

$$m_1 = \sum_{l=1}^{N/2} l \cdot S'(l), \quad (5)$$

$$m_2 = \sum_{l=1}^{N/2} (l - m_1)^2 \cdot S'(l). \quad (6)$$

For the spectra presented in Fig. 8, the values of pairs of m_1 corresponding to the right and left hand, respectively, are [1.53 1.47], [2.40 2.89] and [3.95 4.02] for cases A, B and C. Similarly, the pairs of m_2 calculated for the right and left hand are [3.28 3.51], [3.26 3.61] and [2.67 2.38], respectively.

6.3. Using domain knowledge in feature selection

The rapid Finger Tapping Test is performed for the left and right hands. This means that each patient can be formally described using eight parameters (four of the above described for each hand). In the cases of equally affected sides, this is a redundant description, since the limitation of motor functions affects both the left and right hand. In the case of unilateral symptoms, this is a misleading description, because the motor skills of one of the hands are theoretically the same as in healthy people. For the above reasons, the use of all eight characteristics is pointless and in the analysis presented below it was characterized by a deteriorated generalization ability as compared to the case when the limitation of the number of features to four was applied. The idea of selecting these four features was to compare their numerical values obtained for the left and right hand and then choose the proper one from the point of view of domain knowledge about Parkinson's disease. Thus, in the case of the first spectral moment, which represents the average frequency of movement, a lower value is selected. For the second spectral moment, which represents the broadening of the spectrum due to frequency fluctuations, a higher value is selected. In the case of skewness, which is a measure of the asymmetry of the distribution of the value caused by different times of leaving the fingers in extreme positions, a larger value is also selected. In the case of kurtosis, which is a measure of the shape of the data distribution, due to the irregularity of the finger movement, a higher value should be selected. A summary of the medians of the four characteristics selected by the above method in both populations is presented in Table 2 together with interquartile ranges (iqr) representing the spread of the data. The measures were used as they are robust to outliers.

The relationships between the medians of features in both groups, which are consistent with the knowledge of the rapid Finger Tapping Test, confirm the adopted method of their selection. However, attention should be paid to the relatively large spread of two parameters, namely the skewness and the first spectral moment. Further assessment of the statistical significance in the differentiation of PD and HC groups by all of the proposed parameters was done with the use of the Wilcoxon rank sum test, which verifies the hypothesis of median equality in two independent populations. The results in the form of p-values are presented in Table 2. These results indicate indeed that only in the case of kurtosis and the second-order spectral moment the hypothesis of median equality can be rejected. Thus these features can be assessed as good in the process of differentiation of PD and HC groups. However, the Wilcoxon test evaluates the characteristics in an individual way, without taking into account their possible synergy. In order to maintain the thesis about the legitimacy of using the other two features, we transformed four-dimensional data into one-dimensional

Table 2

Comparison of descriptive statistics of features together with p-values in the Wilcoxon rank sum tests used to evaluate them

	skewness	kurtosis	1 st spectral mom.	2 nd spectral mom.	LDA feature
median ± iqr					
PD	0.50 ± 0.64	1.53 ± 0.51	3.29 ± 1.39	3.44 ± 0.46	0.96 ± 0.32
HC	0.33 ± 0.31	1.42 ± 0.16	3.54 ± 0.64	3.04 ± 0.81	0.50 ± 0.17
results of the Wilcoxon rank sum tests					
p-value	0.279	0.003	0.182	0.005	8.2 · 10 ⁻⁷

space using LDA transform (linear discriminant analysis). The transform is discussed in [24] and its usage as a feature transform can be found in [25]. The new feature obtained with LDA is a linear combination of all four features with the coefficients selected so that in the one-dimensional space between-class distance to the within-class spread ratio is maximized, which guarantees maximal discrimination. The Wilcoxon test performed for this new LDA feature provided a p-value of 8.2 · 10⁻⁷ (see Table 2), which denies the median equality hypothesis more than for each of the features considered separately. For this reason, all four features were used as candidates for the classification task.

7. CLASSIFICATION

In order to check to what extent it is possible to separate the class of healthy people from the class of people with Parkinson's disease by means of features obtained by the above processing of data obtained in the rapid tapping test, a classification process was carried out. Standard methods were used for this purpose, i.e. SVM networks with various kernel functions and the closest neighborhood method (k-NN).

7.1. Methodology of the assessment

Due to the low amount of data, a cross-validation technique was used to avoid the risk of too optimistic and unreliable assessments. In this technique, the available data set is divided into a number of disjoint K-folds of equal size. Each individual fold is treated as test data, while the others are used to train the model. The process is repeated K times so that all data is used in testing and training. However, if a particular fold belongs to the testing data, then it is not used in the training process. The value of K is often set to five or ten, but there is no formal rule for this [11]. In this work, seven-fold cross-validation was used, placing in each fold three samples from the PD and HC groups, i.e. a total of six samples. The results of the recognition, in order to compare with the material presented in the competing works, were expressed by measures *precision*, *recall* (*sensitivity*), *specificity* and *F₁ score*:

$$precision = TP / (TP + FP), \quad (7)$$

$$sensitivity = TP / (TP + FN), \quad (8)$$

$$specificity = TN / (TN + FP), \quad (9)$$

$$F_1 \text{ score} = 2 \cdot TP / (2 \cdot TP + FN + FP). \quad (10)$$

The measures defined by the above equations are taken from the concept of the error matrix [11]. The error matrix is a simple cross table of actual and recognized classes that allows us to easily calculate classifier parameters. Its diagonal cells mean the number *TP* of people correctly classified as sick and the number *TN* of people properly classified as healthy, while the cells outside the diagonal contain the number of people classified in the wrong way. *FP* means healthy cases classified as sick and *FN* stands for patients classified as healthy.

7.2. Results

The results shown in Table 3 refer to the testing and are presented by average values achieved in cross-validation together with confidence intervals. They were obtained while meeting the requirement that the number of errors in the training process should be zero. For this reason, when choosing the number of neighbors in the k-NN method, it was limited only to *k* = 1. There were non-zero classification errors for the training data

Table 3

Performance of different recognition methods

framework	<i>precision</i>	<i>sensitivity</i>	<i>specificity</i>	<i>F₁ score</i>
8 feat. + SVM (cubic kernel)	0.76 ± 0.03	0.66 ± 0.04	0.71 ± 0.05	0.67 ± 0.03
8 feat. + SVM (RBF kernel)	0.71 ± 0.03	0.76 ± 0.05	0.57 ± 0.05	0.67 ± 0.02
8 feat. + 1-NN (Eucl. dist.)	0.68 ± 0.04	0.57 ± 0.04	0.57 ± 0.05	0.67 ± 0.02
8 feat. + 1-NN (Mahal. dist.)	0.74 ± 0.03	0.57 ± 0.05	0.57 ± 0.06	0.57 ± 0.03
4 feat. + SVM (cubic kernel)	0.83 ± 0.02	0.71 ± 0.03	0.81 ± 0.03	0.74 ± 0.02
4 feat. + SVM (RBF kernel)	0.77 ± 0.03	0.81 ± 0.04	0.76 ± 0.02	0.78 ± 0.03
4 feat. + 1-NN (Eucl. dist.)	0.70 ± 0.05	0.71 ± 0.05	0.81 ± 0.03	0.69 ± 0.04
4 feat. + 1-NN (Mahal. dist.)	0.84 ± 0.03	0.71 ± 0.04	0.81 ± 0.04	0.73 ± 0.03

when $k > 1$. In the SVM method, a polynomial kernel of order 3 seems to be optimal because kernels of orders different from that caused an increase in testing errors.

The feature vectors were normalized by centering and dividing the value of their elements by standard deviations of the training data. As can be seen, the most common measures used by physicians, i.e. sensitivity and specificity can reach the level of 80%. In order to verify which of the classifiers distinguished in Table 3 is characterized by better properties, ROC curves have been determined for them.

The curves are depicted in Fig. 9 and AUC measures that are equal to 0.68 for the SVM with RBF kernel and 0.79 for SVM with the polynomial cubic kernel, show a significantly better performance of the latter.

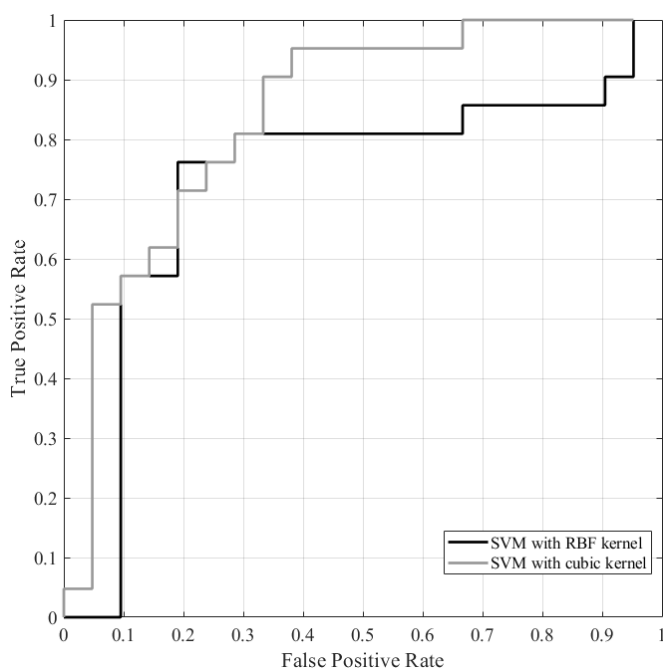


Fig. 9. ROC curves for two the most promising classifiers

8. CONCLUSIONS

The presented material discusses the possibilities of using relatively simple methods of image acquisition and processing as well as machine learning algorithms in the process of objectification of one of the tests of motor functions, used in the clinical practice of medical diagnosis of patients with possible Parkinson's disease. There was no need to use a motion capture system or advanced processing to successfully quantify the rapid Finger Tapping Test. The obtained results are similar to the achievements discussed in comparable papers devoted to the use of a similar idea of image data acquisition. A novelty of this article is the proposal to transfer the decision about which hand is to be used to generate the diagnostic features necessary to carry out the classification process to the algorithm of processing. It should also be emphasized that our results are the result of research conducted in a group of PD patients in the ON phase. For this reason, it seems that they are characterized

by the greater potential for the development of new diagnostic methods different from those used during medical history. The medical interview commonly uses methods of a patient's evaluation validated in the OFF phase, i.e. in the phase in which the symptoms of the disease are clearly visible to the naked eye.

A certain limitation of our study is the not very large number of people taking part in the experiment, although it is similar to the number of people taking part in the research reported in the most advanced and comparable paper [14]. The data presented in Table 1 are rather specific taking into account age and gender; however, in clinical practice, they are also not taken into account in the formal assessment of a patient's condition using the UPDRS scale. A larger sample size would be needed to determine the reliability of classification methods more fully. In addition, we show a merely binary classification approach without any granularity of information to rate the disease severity. However, the proposed method of image acquisition seems to be simple enough to collect the right amount of data for the needs of future studies.

ACKNOWLEDGEMENTS

This work was financed by the Military University of Technology under research project UGB 865.

REFERENCES

- [1] A. Berardelli, J.C. Rothwell, P.D. Thompson, and M. Hallett, "Pathophysiology of bradykinesia in Parkinson's disease," *Brain*, vol. 124, no. 11, pp. 2131–2146, 2001, doi: [10.1093/brain/124.11.2131](https://doi.org/10.1093/brain/124.11.2131).
- [2] J.A. Obeso, "The Unified Parkinson's Disease Rating Scale (UPDRS): Status and recommendations," *Mov. Disord.*, vol. 18, pp. 738–750, 2003.
- [3] International Parkinson and Movement Disorder Society. "MDS Rating Scales." [Online]. Available: <https://www.movementdisorders.org/MDS/MDS-Rating-Scales/MDS-Unified-Parkinsons-Disease-Rating-Scale-MDS-UPDRS.htm> [Accessed: 19 Feb. 2023].
- [4] W. Chen *et al.*, "A Survey on Hand Pose Estimation with Wearable Sensors and Computer-Vision-Based Methods," *Sensors*, vol. 20, p. 1074, 2020, doi: [10.3390/s20041074](https://doi.org/10.3390/s20041074).
- [5] M. Djuric-Jovicic, N. Jovičić, A. Roby-Brami, M. Popović, V. Kostić, and A. Djordjevic, "Quantification of Finger-Tapping Angle Based on Wearable Sensors," *Sensors*, vol. 17, no. 203, 2017, doi: [10.3390/s17020203](https://doi.org/10.3390/s17020203).
- [6] V. Bobić, M. Djurić-Jovičić, N. Dragašević, M. Popović, V. Kostić, and G. Kvaščev, "An Expert System for Quantification of Bradykinesia Based on Wearable Inertial Sensors," *Sensors*, vol. 19, no. 11, p. 2644, 2019, doi: [10.3390/s19112644](https://doi.org/10.3390/s19112644).
- [7] M. Monje, G. Foffani, J. Obeso, and Á. Sánchez-Ferro, "New Sensor and Wearable Technologies to Aid in the Diagnosis and Treatment Monitoring of Parkinson's Disease," *Annu. Rev. Biomed. Eng.*, vol. 4, no. 21, pp. 111–143, 2019, doi: [10.1146/annurev-bioeng-062117-121036](https://doi.org/10.1146/annurev-bioeng-062117-121036).
- [8] S. Jomyo, A. Furui, T. Matsumoto, T. Tsunoda, and T. Tsuji, "A Wearable Finger-Tapping Motion Recognition System Using Biodegradable Piezoelectric Film Sensors," in *Proc. 43rd Annual International Conference of the IEEE Engineering in Medicine & Biology Society (EMBC)*, 2021, pp. 6982–6986, doi: [10.1109/EMBC46164.2021.9630643](https://doi.org/10.1109/EMBC46164.2021.9630643).

Application of imaging techniques to objectify *Finger Tapping Test* used in the diagnosis of Parkinson's disease

- [9] R. Krupicka, Z. Szabo, and M. Jirina, "Motion Camera System for Measuring Finger Tapping in Parkinson's Disease," in *Proc. 5th European Conference of the International Federation for Medical and Biological Engineering (IFMBE)*, 2011, doi: [10.1007/978-3-642-23508-5_220](https://doi.org/10.1007/978-3-642-23508-5_220).
- [10] C. Lainscsek *et al.*, "Finger tapping movements of Parkinson's disease patients automatically rated using nonlinear delay differential equations," *Chaos*, vol. 22, p. 3444, 2012, doi: [10.1063/1.3683444](https://doi.org/10.1063/1.3683444).
- [11] M. Kuhn and K. Johnson. *Applied predictive modeling*. New York: Springer, 2013, doi: [10.1007/978-1-4614-6849-3](https://doi.org/10.1007/978-1-4614-6849-3).
- [12] T. Khan, D. Nyholm, J. Westin, and M. Dougherty, "A computer vision framework for finger-tapping evaluation in Parkinson's disease," *Artif. Intell. Med.*, vol. 60, no. 1, pp. 27–40, 2014, doi: [10.1016/j.artmed.2013.11.004](https://doi.org/10.1016/j.artmed.2013.11.004).
- [13] K. Bialek *et al.*, "Selected problems of image data preprocessing used to perform examination in Parkinson's disease," *Proc. SPIE 11442, Radioelectronic Systems Conference*, 2019, p. 114420G, doi: [10.1117/12.2565138](https://doi.org/10.1117/12.2565138).
- [14] M. Monje *et al.*, "Remote Evaluation of Parkinson's Disease Using a Conventional Webcam and Artificial Intelligence," *Front. Neurol.*, vol. 23, no. 12, 2021, doi: [10.3389/fneur.2021.742654](https://doi.org/10.3389/fneur.2021.742654).
- [15] S. Bambach, S. Lee, D.J. Crandall, and C. Yu, "Lending A Hand: Detecting Hands and Recognizing Activities in Complex Egocentric Interactions," in *Proc. IEEE International Conference on Computer Vision (ICCV)*, 2015, pp. 1949–1957, doi: [10.1109/ICCV.2015.226](https://doi.org/10.1109/ICCV.2015.226).
- [16] Z. Cao, G. Hidalgo, T. Simon, S. -E. Wei, and Y. Sheikh, "OpenPose: Realtime Multi-Person 2D Pose Estimation Using Part Affinity Fields," in *IEEE Trans. Pattern Anal. Mach. Intell.*, 2021, vol. 43, no. 1, pp. 172–186, doi: [10.1109/TPAMI.2019.2929257](https://doi.org/10.1109/TPAMI.2019.2929257).
- [17] B. Das, K. Daoudi, J. Klempir, and J. Ruzs, "Towards disease-specific speech markers for differential diagnosis in parkinsonism," in *Proceedings of the IEEE International Conference on Acoustics, Speech and Signal Processing*, 2019, pp. 5846–5850.
- [18] E. Majda-Zdancewicz, A. Potulska-Chromik, J. Jakubowski, M. Nojszewska, and A. Kostera-Pruszczyk, "Deep Learning vs. Feature Engineering in the Assessment of Voice Signals for Diagnosis in Parkinson's Disease," *Bull. Pol. Acad. Sci. Tech. Sci.*, vol. 69, p. e137347, 2021, doi: [10.24425/bpasts.2021.137347](https://doi.org/10.24425/bpasts.2021.137347).
- [19] F. Amato, L. Borzi, G. Olmo, and J.R. Orozco-Arroyave, "An algorithm for Parkinson's disease speech classification based on isolated words analysis," *Health Inf. Sci. Syst.*, vol. 9, p. 32, 2021, doi: [10.1007/s13755-021-00162-8](https://doi.org/10.1007/s13755-021-00162-8).
- [20] J. Carrón, Y. Campos-Roca, M. Madruga, and C.J. Perez, "A mobile-assisted voice condition analysis system for Parkinson's disease: assessment of usability conditions," *Biomed. Eng. On-Line*, vol. 20, p. 114, 2021, doi: [10.1186/s12938-021-00951-y](https://doi.org/10.1186/s12938-021-00951-y).
- [21] M.T. Angelillo, D. Impedovo, G. Pirlo, and G. Vessio, "Performance-Driven Handwriting Task Selection for Parkinson's Disease Classification," in *Lecture Notes in Computer Science*, vol. 11946, 2019, doi: [10.1007/978-3-030-35166-3_20](https://doi.org/10.1007/978-3-030-35166-3_20).
- [22] C.D. Rios-Urregoa, J.C. Vázquez-Correaab, J.F. Vargas-Bonillaa, E. Nöthb, F. Loperac, and J.R. Orozco-Arroyaveab, "Analysis and evaluation of handwriting in patients with Parkinson's disease using kinematic, geometrical, and non-linear features," *Comput. Meth. Programs Biomed.*, vol. 173, 2019, pp. 43–52, doi: [10.1016/j.cmpb.2019.03.005](https://doi.org/10.1016/j.cmpb.2019.03.005).
- [23] F. Vogel, S. Holm, and O.C. Lingjærde, "Spectral moments and time domain representation of photoacoustic signals used for detection of crude oil in produced water," in *Proc. Norwegian Signal Processing. Conf. (NORSIG-01)*, 2001.
- [24] Y. Qiu, G. Zhou, Q. Zhao, and A. Cichocki, "Comparative study on the classification methods for breast cancer diagnosis," *Bull. Pol. Acad. Sci. Tech. Sci.*, vol. 66, no 6, pp. 841–848, 2018, doi: [10.24425/bpas.2018.125931](https://doi.org/10.24425/bpas.2018.125931).
- [25] W. Yunzhu and C. Yunli, "A new feature extraction algorithm based on Fisher linear discriminant analysis," in *Proc. International Conference on Control, Automation and Robotics (IC-CAR)*, 2017, pp. 24–26, doi: [10.1109/ICCAR.2017.7942729](https://doi.org/10.1109/ICCAR.2017.7942729).